

Supporting Information

Hirsutinolide series inhibit Stat3 activity, alter GCN1, MAP1B, Hsp105, G6PD, vimentin and importin α -2 expression, and induce antitumor effects against human glioma

Gabriella Miklossy^{1,2}, Ui Joung Youn³, Peibin Yue^{1,2}, Mingming Zhang³, Chih-Hong Chen⁴, Tyvette S. Hilliard^{1,2}, David Paladino^{1,2}, Yifei Li⁴, Justin Choi⁴, Jann N. Sarkaria⁵, Joel K. Kawakami⁶, Supakit Wongwiwatthananut³, Yuan Chen⁴, Dianqing Sun³, Leng Chee Chang³, and James Turkson^{1,2,*}

¹Natural Products and Experimental Therapeutics and ²Cancer Biology Programs, University of Hawaii Cancer Center, University of Hawaii at Manoa, Honolulu, HI, ³Department of Pharmaceutical Sciences, The Daniel K. Inouye College of Pharmacy, University of Hawaii at Hilo, Hilo, HI, ⁴Department of Molecular Medicine, Beckman Research Institute of the City of Hope, Duarte, CA, ⁵Department of Radiation Oncology, Mayo Clinic, Rochester, MN, ⁶Division of Natural Sciences and Mathematics, Chaminade University, Honolulu, HI

Content:

Materials and Methods

Figures and Figure Legends

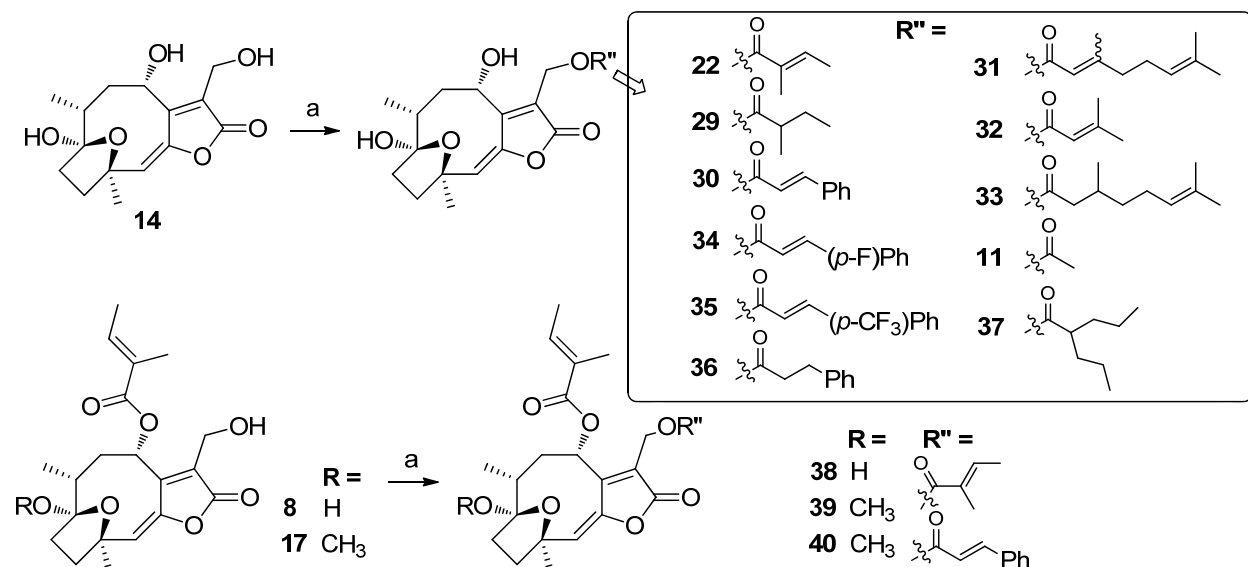
Keywords: Natural products, hirsutinolides, Stat3, glioma, xenografts, antitumor effects, GCN1, Vimentin and importin α -2, microtubule-associated protein 1B; thioredoxin reductase 1 cytoplasmic isoform 3; glucose-6-phosphate 1-dehydrogenase isoform a; heat shock protein105; and tumor necrosis factor α -induced protein 2.

Materials and Methods

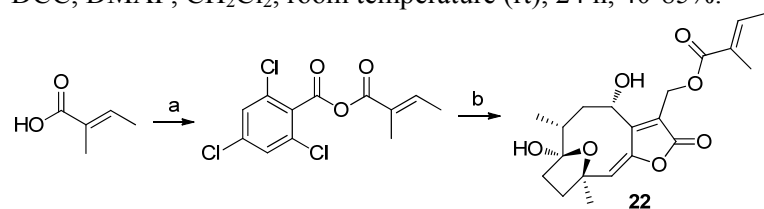
All reagents and solvents were purchased from commercial sources and used without further purification.

Semi-synthesis of natural product analogs

We performed re-synthesis of **22** or the semi-synthesis of its analogs using **14**, **8**, or **17** as a starting material to expand the existing SAR of isolated natural hirsutinolides (Scheme 1). This was accomplished by reacting the isolated major natural product components, **14**, **8** or **17** with a selected panel of carboxylic acids in the presence of dicyclohexylcarbodiimide (DCC) and catalytic amounts of 4-(dimethylamino)pyridine (DMAP) by conventional Steglich esterification¹, affording the desired semi-synthetic derivatives in 40-85% yields. Due to the difficulty in removing the dicyclohexylurea byproduct and to further facilitate the purification process, Yamaguchi esterification protocol was employed to scale-up semi-synthesis of compound **22**². Briefly, the Yamaguchi mixed anhydride was generated *in situ* from 2,4,6-trichlorobenzoyl chloride and tiglic acid³, followed by the treatment with **14** in the presence of catalytic DMAP in toluene to afford **22** in 78% yield (Scheme 2). Title compounds were purified by normal phase column chromatography, preparative TLC, and/or semi-preparative reverse phase HPLC. The spectroscopic data of our semi-synthetic **22** are in full agreement with those of isolated natural products⁴.



Scheme S1. Semi-synthesis of hirsutinolide derivatives. (a) Appropriate carboxylic acid ($\text{R}''\text{COOH}$), DCC, DMAP, CH_2Cl_2 , room temperature (rt), 24 h, 40-85%.



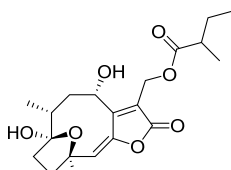
Scheme S2. Scale-up semi-synthesis of **22**. (a) 2,4,6-trichlorobenzoyl chloride, diisopropylethylamine (DIPEA), toluene, rt, 5 h, 32%. (b) **14**, DMAP, toluene, 50 °C, 24 h, 78%.

General information

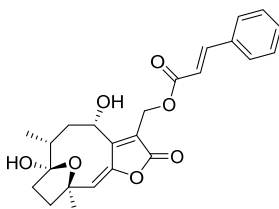
Solvents and reagents were purchased from Sigma-Aldrich and Fisher Scientific and were used without further purification. All reactions were monitored by either TLC or HPLC (Shimadzu LC-20A series system). Compounds were purified by flash column chromatography on silica gel using a Biotage Isolera One system, preparative silica gel TLC plate (w/UV254, glass backed, 500 μm , 20 \times 20 cm; Sorbent Technologies), and/or semi-preparative reverse phase HPLC. Proton nuclear magnetic resonance (^1H NMR) spectra were recorded employing a Bruker AVANCE (400 MHz) spectrometer. Chemical shifts were expressed in parts per million (ppm), J values were in Hertz. Mass spectra were recorded on a Varian 500-MS IT mass spectrometer using ESI. The purity of compounds was determined by analytical HPLC (Shimadzu LC-20A series) using a Gemini, 3 μM , C18, 110 \AA column (50 mm \times 4.6 mm, Phenomenex) and flow rate of 1 mL/min. Gradient conditions: solvent A (0.1% trifluoroacetic acid in water) and solvent B (acetonitrile): 0-2.0 min 100% A, 2.0-7.0 min 0-100% B (linear gradient), 7.0-8.0 min 100% B. UV detection at 254 nm and 284 nm. All the tested compounds were obtained with $\geq 96.0\%$ purity by HPLC.

General procedure for the semi-synthesis of hirsutinolide derivatives

To a stirred solution of **14**, **8**, or **17** (0.0068 mmol) in anhydrous CH_2Cl_2 (2 mL) was added DMAP (0.42 mg, 0.0034 mmol) and appropriate carboxylic acid (0.0136 mmol). DCC (2.81 mg, 0.0136 mmol) was added to the reaction at 0 $^\circ\text{C}$ and the reaction mixture was then stirred for 5 min at 0 $^\circ\text{C}$ and 24 h at room temperature. The residue was purified by preparative TLC (Hexane-Ethyl Acetate as developing solvent) and/or semi-preparative reverse phase HPLC to give desired target compounds in 40-85% yields.

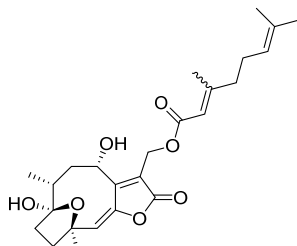


(29) ((4S,6R,E)-4,7-dihydroxy-6,10-dimethyl-2-oxo-2,4,5,6,7,8,9,10-octahydro-7,10-epoxycyclodeca[b]furan-3-yl)methyl 2-methylbutanoate. White amorphous powder (2.17 mg, 84%); ^1H NMR (400 MHz, CDCl_3) δ 6.15 (d, J = 11.5 Hz, 1H), 5.88 (s, 1H), 5.17 (dd, J = 12.4, 6.1 Hz, 1H), 4.98 – 4.86 (m, 2H), 2.52 (s, 1H), 2.45 – 2.39 (m, 1H), 2.36 (d, J = 7.7 Hz, 1H), 2.31 – 2.21 (m, 3H), 2.11 – 2.07 (m, 1H), 1.87 (dd, J = 15.8, 7.0 Hz, 2H), 1.69 (s, 2H), 1.63 (s, 3H), 1.17 (dd, J = 7.0, 1.2 Hz, 3H), 0.99 (d, J = 6.9 Hz, 3H), 0.93 (t, J = 8.0 Hz, 3H). LRMS (ES+) calculated for $[\text{C}_{20}\text{H}_{28}\text{O}_7 + \text{Na}]$ 403.2, found 403.4. HPLC purity: 99.2% (254 nm), t_R : 6.54 min, 99.2% (284 nm), t_R : 6.54 min.

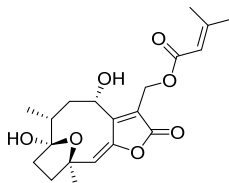


(30) ((4S,6R,E)-4,7-dihydroxy-6,10-dimethyl-2-oxo-2,4,5,6,7,8,9,10-octahydro-7,10-epoxycyclodeca[b]furan-3-yl)methyl cinnamate. White amorphous powder (2.46 mg, 85%); ^1H NMR (400 MHz, CDCl_3) δ 7.74 (d, J = 16.0 Hz, 1H), 7.53 (dd, J = 6.8, 2.9 Hz, 2H), 7.46 – 7.36 (m, 3H), 6.44 (d, J = 16.0 Hz, 1H), 6.19 (d, J = 11.8 Hz, 1H), 5.89 (s, 1H), 5.30 – 5.19 (m,

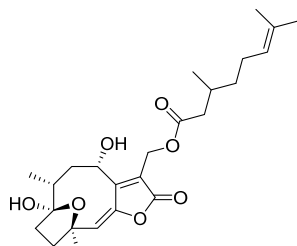
1H), 5.06 (s, 2H), 2.65 (s, 1H), 2.32 – 2.16 (m, 4H), 2.11 – 2.03 (m, 1H), 1.95 (dd, $J = 12.1$, 6.9 Hz, 1H), 1.92 – 1.84 (m, 1H), 1.63 (s, 3H), 0.97 (d, $J = 6.8$ Hz, 3H). LRMS (ES+) calculated for $[C_{24}H_{26}O_7 + Na]$ 449.2, found 449.1. HPLC purity: 97.1% (254 nm), t_R : 6.72 min, 97.7% (284 nm), t_R : 6.54 min.



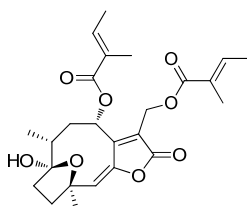
(31) ((4S,6R,E)-4,7-dihydroxy-6,10-dimethyl-2-oxo-2,4,5,6,7,8,9,10-octahydro-7,10-epoxycyclodeca[b]furan-3-yl)methyl 3,7-dimethylocta-2,6-dienoate. White amorphous powder (1.37 mg, 45%); 1H NMR (400 MHz, $CDCl_3$) δ 6.16 (t, $J = 12.1$ Hz, 1H), 5.87 (d, $J = 11.0$ Hz, 1H), 5.24 – 5.04 (m, 2H), 4.98 – 4.87 (m, 2H), 2.31 – 2.05 (m, 10H), 2.00 – 1.92 (m, 2H), 1.92 – 1.82 (m, 2H), 1.70 (s, 3H), 1.63 (d, $J = 6.8$ Hz, 6H), 0.98 (t, $J = 7.3$ Hz, 3H). LRMS (ES+) calculated for $[C_{25}H_{34}O_7 + Na]$ 469.2, found 469.5. HPLC purity: 99.8% (254 nm), t_R : 7.21 min, 99.9% (284 nm), t_R : 7.21 min.



(32) ((4S,6R,E)-4,7-dihydroxy-6,10-dimethyl-2-oxo-2,4,5,6,7,8,9,10-octahydro-7,10-epoxycyclodeca[b]furan-3-yl)methyl 3-methylbut-2-enoate. White amorphous powder (1.26 mg, 49%); 1H NMR (400 MHz, $CDCl_3$) δ 6.14 (d, $J = 11.8$ Hz, 1H), 5.86 (s, 1H), 5.70 – 5.64 (m, 1H), 5.24 – 5.16 (m, 1H), 4.98 – 4.88 (m, 2H), 2.60 (s, 1H), 2.30 – 2.11 (m, 6H), 2.11 – 2.04 (m, 1H), 2.01 – 1.79 (m, 6H), 1.62 (s, 3H), 0.97 (d, $J = 6.8$ Hz, 3H). LRMS (ES+) calculated for $[C_{20}H_{26}O_7 + Na]$ 401.2, found 401.4. HPLC purity: 97.9% (254 nm), t_R : 6.43 min, 99.4% (284 nm), t_R : 6.43 min.

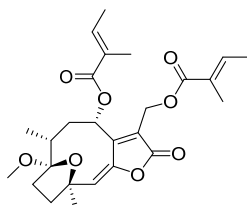


(33) ((4S,6R,E)-4,7-dihydroxy-6,10-dimethyl-2-oxo-2,4,5,6,7,8,9,10-octahydro-7,10-epoxycyclodeca[b]furan-3-yl)methyl 3,7-dimethyloct-6-enoate. White amorphous powder (2.34 mg, 77%); 1H NMR (400 MHz, $CDCl_3$) δ 6.17 (d, $J = 11.6$ Hz, 1H), 5.88 (s, 1H), 5.24 – 5.12 (m, 1H), 5.09 (dd, $J = 7.7$, 6.4 Hz, 1H), 4.97 – 4.85 (m, 2H), 2.65 (s, 1H), 2.41 – 1.80 (m, 13H), 1.70 (d, $J = 1.0$ Hz, 4H), 1.62 (s, 3H), 1.61 (s, 4H), 0.99 (d, $J = 6.8$ Hz, 3H), 0.96 (d, $J = 6.6$ Hz, 3H). LRMS (ES+) calculated for $[C_{25}H_{36}O_7 + Na]$ 471.2, found 471.4. HPLC purity: 98.9% (254 nm), t_R : 7.26 min, 98.8% (284 nm), t_R : 7.26 min.



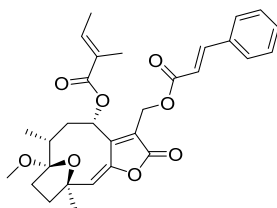
(38) (4S,6R,E)-7-hydroxy-6,10-dimethyl-3-(((E)-2-methylbut-2-enoyloxy)methyl)-2-oxo-2,4,5,6,7,8,9,10-octahydro-7,10-epoxycyclodeca[b]furan-4-yl (E)-2-methylbut-2-enoate.

White amorphous powder (1.25 mg, 40%); ^1H NMR (400 MHz, CD_3OD) δ 7.13 (dd, $J = 7.1, 1.5$ Hz, 1H), 6.93 (dd, $J = 7.0, 1.4$ Hz, 1H), 6.28 (d, $J = 7.6$ Hz, 1H), 6.04 (s, 1H), 5.14 (d, $J = 13.0$ Hz, 1H), 5.01 (d, $J = 12.9$ Hz, 1H), 2.40 (dd, $J = 16.2, 12.2$ Hz, 1H), 2.12 (dd, $J = 11.5, 5.6$ Hz, 2H), 1.92 – 1.84 (m, 9H), 1.84 – 1.79 (m, 6H), 1.75 (s, 1H), 1.49 (s, 3H), 0.88 (d, $J = 6.9$ Hz, 3H). LRMS (ES+) calculated for $[\text{C}_{25}\text{H}_{32}\text{O}_8 + \text{Na}]$ 483.2, found 483.4. HPLC purity: 99.7% (254 nm), t_{R} : 7.14 min, 99.7% (284 nm), t_{R} : 7.14 min.



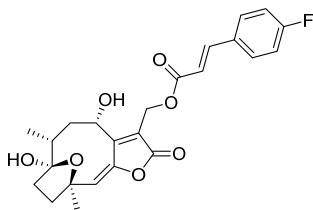
(39) (4S,6R,E)-7-methoxy-6,10-dimethyl-3-(((E)-2-methylbut-2-enoyloxy)methyl)-2-oxo-2,4,5,6,7,8,9,10-octahydro-7,10-epoxycyclodeca[b]furan-4-yl (E)-2-methylbut-2-enoate.

White amorphous powder (1.35 mg, 42%); ^1H NMR (400 MHz, CDCl_3) δ 7.05 (dd, $J = 7.1, 1.5$ Hz, 1H), 6.95 – 6.84 (m, 1H), 6.27 (d, $J = 7.6$ Hz, 1H), 5.87 (s, 1H), 5.20 (d, $J = 13.1$ Hz, 1H), 5.07 (d, $J = 12.9$ Hz, 1H), 3.29 (s, 3H), 2.38 (dd, $J = 15.6, 11.9$ Hz, 1H), 2.23 – 2.07 (m, 2H), 2.02 – 1.86 (m, 3H), 1.84 (dt, $J = 2.6, 1.3$ Hz, 6H), 1.80 (dd, $J = 7.1, 1.1$ Hz, 6H), 1.76 (d, $J = 10.0$ Hz, 1H), 1.51 (s, 3H), 0.86 (d, $J = 7.0$ Hz, 3H). LRMS (ES+) calculated for $[\text{C}_{26}\text{H}_{34}\text{O}_8 + \text{Na}]$ 497.2, found 497.5. HPLC purity: 99.8% (254 nm), t_{R} : 7.76 min, 99.8% (284 nm), t_{R} : 7.76 min.

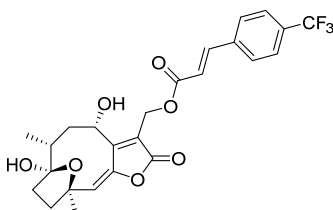


(40) (4S,6R,E)-3-((cinnamoyloxy)methyl)-7-methoxy-6,10-dimethyl-2-oxo-2,4,5,6,7,8,9,10-octahydro-7,10-epoxycyclodeca[b]furan-4-yl (E)-2-methylbut-2-enoate.

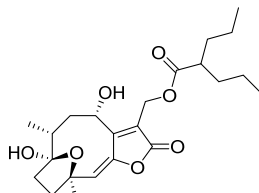
White amorphous powder (2.91 mg, 82%); ^1H NMR (400 MHz, CDCl_3) δ 7.73 (d, $J = 16.0$ Hz, 1H), 7.53 (dd, $J = 6.7, 2.9$ Hz, 2H), 7.45 – 7.37 (m, 3H), 7.06 (dd, $J = 7.1, 1.5$ Hz, 1H), 6.43 (d, $J = 16.0$ Hz, 1H), 6.34 (d, $J = 7.8$ Hz, 1H), 5.90 (s, 1H), 5.30 (d, $J = 13.0$ Hz, 1H), 5.14 (d, $J = 12.9$ Hz, 1H), 3.29 (s, 3H), 2.41 (dd, $J = 15.8, 11.3$ Hz, 1H), 2.23 – 2.06 (m, 2H), 1.95 (ddd, $J = 16.9, 15.8, 9.5$ Hz, 3H), 1.85 (dd, $J = 5.8, 4.5$ Hz, 4H), 1.80 (dd, $J = 7.1, 1.1$ Hz, 3H), 1.51 (s, 3H), 0.87 (d, $J = 6.9$ Hz, 3H). LRMS (ES+) calculated for $[\text{C}_{30}\text{H}_{34}\text{O}_8 + \text{Na}]$ 545.2, found 545.2. HPLC purity: 96.0% (254 nm), t_{R} : 7.88 min, 97.5% (284 nm), t_{R} : 7.88 min.



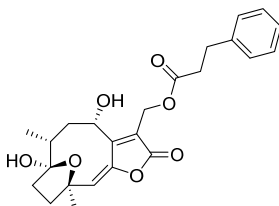
(34) ((4*S*,6*R*,*E*)-4,7-dihydroxy-6,10-dimethyl-2-oxo-2,4,5,6,7,8,9,10-octahydro-7,10-epoxycyclodeca[*b*]furan-3-yl)methyl (*E*)-3-(4-fluorophenyl)acrylate. White amorphous powder (1.6 mg, 53%); ^1H NMR (400 MHz, CDCl_3) δ 7.69 (d, $J = 16.0$ Hz, 1H), 7.58 – 7.46 (m, 2H), 7.10 (t, $J = 8.6$ Hz, 2H), 6.36 (d, $J = 16.0$ Hz, 1H), 6.17 (d, $J = 11.8$ Hz, 1H), 5.90 (s, 1H), 5.29 – 5.20 (m, 1H), 5.05 (s, 2H), 2.59 (s, 1H), 2.33 – 2.16 (m, 4H), 2.11 – 2.03 (m, 1H), 1.95 (dd, $J = 12.1, 6.8$ Hz, 1H), 1.91 – 1.83 (m, 1H), 1.63 (s, 3H), 0.97 (d, $J = 6.8$ Hz, 3H). LRMS (ES+) calculated for $[\text{C}_{24}\text{H}_{25}\text{FO}_7 + \text{Na}]$ 467.1, found 467.1. HPLC purity: 96.4% (254 nm), t_R : 6.77 min, 97.2% (284 nm), t_R : 6.77 min.



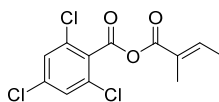
(35) ((4*S*,6*R*,*E*)-4,7-dihydroxy-6,10-dimethyl-2-oxo-2,4,5,6,7,8,9,10-octahydro-7,10-epoxycyclodeca[*b*]furan-3-yl)methyl (*E*)-3-(4-(trifluoromethyl)phenyl)acrylate. White amorphous powder (1.6 mg, 48%); ^1H NMR (400 MHz, CDCl_3) δ 7.74 (d, $J = 16.0$ Hz, 1H), 7.65 (q, $J = 8.5$ Hz, 4H), 6.51 (d, $J = 16.0$ Hz, 1H), 6.19 (d, $J = 11.8$ Hz, 1H), 5.91 (s, 1H), 5.25 (dd, $J = 11.8, 5.4$ Hz, 1H), 5.07 (s, 2H), 2.58 (s, 1H), 2.34 – 2.15 (m, 4H), 2.13 – 2.03 (m, 1H), 1.96 (dd, $J = 13.3, 5.9$ Hz, 1H), 1.92 – 1.82 (m, 1H), 1.63 (s, 3H), 0.98 (d, $J = 6.8$ Hz, 3H). LRMS (ES+) calculated for $[\text{C}_{25}\text{H}_{25}\text{F}_3\text{O}_7 + \text{Na}]$ 517.1, found 517.1. HPLC purity: 96.3% (254 nm), t_R : 7.04 min, 96.3% (284 nm), t_R : 7.04 min.



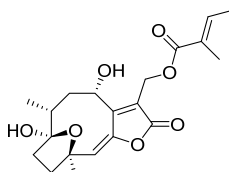
(37) ((4*S*,6*R*,*E*)-4,7-dihydroxy-6,10-dimethyl-2-oxo-2,4,5,6,7,8,9,10-octahydro-7,10-epoxycyclodeca[*b*]furan-3-yl)methyl 2-propylpentanoate. White amorphous powder (1.4 mg, 49%); ^1H NMR (400 MHz, CDCl_3) δ 6.16 (d, $J = 11.8$ Hz, 1H), 5.89 (s, 1H), 5.21 – 5.12 (m, 1H), 4.91 (dd, $J = 30.8, 12.9$ Hz, 2H), 2.58 (s, 1H), 2.45 – 2.34 (m, 1H), 2.24 (ddd, $J = 15.7, 13.0, 10.7$ Hz, 3H), 2.11 – 2.03 (m, 1H), 1.92 (ddd, $J = 15.7, 9.4, 5.5$ Hz, 2H), 1.63 (s, 3H), 1.44 (dddd, $J = 10.5, 7.7, 6.6, 4.0$ Hz, 2H), 1.36 – 1.23 (m, 6H), 1.00 (d, $J = 6.8$ Hz, 2H), 0.91 (td, $J = 7.3, 1.2$ Hz, 6H). LRMS (ES+) calculated for $[\text{C}_{23}\text{H}_{34}\text{O}_7 + \text{Na}]$ 445.2, found 445.1. HPLC purity: 99.0% (254 nm), t_R : 7.09 min, 99.0% (284 nm), t_R : 7.09 min.



(36) ((4*S*,6*R*,*E*)-4,7-dihydroxy-6,10-dimethyl-2-oxo-2,4,5,6,7,8,9,10-octahydro-7,10-epoxycyclodeca[*b*]furan-3-yl)methyl 3-phenylpropanoate. White amorphous powder (2.0 mg, 69%); ^1H NMR (400 MHz, CDCl_3) δ 7.34 – 7.17 (m, 5H), 6.15 (d, J = 11.8 Hz, 1H), 5.88 (s, 1H), 5.17 – 5.08 (m, 1H), 4.91 (s, 2H), 2.97 (t, J = 7.7 Hz, 2H), 2.66 (dd, J = 8.4, 7.2 Hz, 2H), 2.57 (s, 1H), 2.28 – 2.15 (m, 4H), 2.10 – 2.02 (m, 1H), 1.90 (dd, J = 10.9, 5.8 Hz, 1H), 1.78 (ddd, J = 15.9, 6.9, 2.4 Hz, 1H), 1.62 (s, 3H), 0.96 (d, J = 6.8 Hz, 3H). LRMS (ES+) calculated for $[\text{C}_{24}\text{H}_{28}\text{O}_7 + \text{Na}]$ 451.2, found 451.1. HPLC purity: 98.9% (254 nm), t_R : 6.68 min, 98.9% (284 nm), t_R : 6.68 min.



(*E*)-2,4,6-trichlorobenzoyl (*E*)-2-methylbut-2-enoic anhydride. To a premixed solution of tiglic acid (300 mg, 3.0 mmol) and diisopropylethylamine (DIPEA, 0.62 mL, 3.6 mmol) in CH_2Cl_2 (15 mL) was added 2,4,6-trichlorobenzoyl chloride (0.61 mL, 3.6 mmol) dropwise at 0 °C. The resulting solution was stirred at room temperature for 5 h. Dry ether (20 mL) was then added to precipitate DIPEA hydrochloride, followed by the filtration. The filtrate solution was concentrated and the residue was purified by flash column chromatography (1 : 3, CH_2Cl_2 : hexanes) to afford the mixed anhydride as a white crystalline solid (293 mg, 32%). ^1H NMR (400 MHz, CDCl_3) δ 7.43 – 7.36 (m, 2H), 7.17 – 7.10 (m, 1H), 1.91 (dd, J = 2.2, 0.9 Hz, 3H), 1.91 – 1.88 (m, 3H). HPLC purity: 98.4% (254 nm), t_R : 7.55 min, 98.7% (284 nm), t_R : 7.55 min.



(22) ((4*S*,6*R*,*E*)-4,7-dihydroxy-6,10-dimethyl-2-oxo-2,4,5,6,7,8,9,10-octahydro-7,10-epoxycyclodeca[*b*]furan-3-yl)methyl (*E*)-2-methylbut-2-enoate. To a solution of **14** (18 mg, 0.061 mmol) in toluene (2 mL) was added DMAP (3.7 mg, 0.035 mmol) at room temperature. A solution of (*E*)-2,4,6-trichlorobenzoyl (*E*)-2-methylbut-2-enoic anhydride (37.3 mg, 0.122 mmol) in toluene (1 mL) was next added, the reaction was heated at 80 °C for 24 h. After cooling to room temperature, the reaction mixture was concentrated under reduced pressure and purified by flash column chromatography on silica gel (1: 5 to 1 : 2, ethyl acetate : hexanes), affording the title compound **22** as a white solid (19.6 mg, 85%). ^1H NMR (400 MHz, CDCl_3) δ 6.89 (qd, J = 7.0, 1.4 Hz, 1H), 6.15 (d, J = 11.8 Hz, 1H), 5.87 (s, 1H), 5.19 (ddd, J = 11.8, 6.8, 1.4 Hz, 1H), 4.97 (s, 2H), 2.25 (dd, J = 9.1, 6.7 Hz, 1H), 2.20 (d, J = 3.0 Hz, 1H), 2.18 (t, J = 5.0 Hz, 1H), 2.10 – 2.05 (m, 1H), 1.97 – 1.89 (m, 1H), 1.89 – 1.85 (m, 1H), 1.86 – 1.83 (m, 3H), 1.81 (dd, J = 7.1, 1.1 Hz, 3H), 1.62 (s, 3H), 0.96 (d, J = 6.8 Hz, 3H). LRMS (ES+) calculated for $[\text{C}_{20}\text{H}_{26}\text{O}_7 + \text{Na}]$ 401.2, found 401.4. HPLC purity: 99.4% (254 nm), t_R : 6.42 min, 99.2% (284 nm), t_R : 6.42 min.

References

1. Neises B, Steglich W: Simple method for the esterification of carboxylic acids. *Angew Chem Int Ed Engl* **1978**, 17:522-524
2. Inanaga J, Hirata K, Saeki H, Katsuki T, Yamaguchi M: A rapid esterification by means of mixed anhydride and its application to large-ring lactonization. *Bull Chem Soc Jpn* **1979**, 52:1989-1993
3. Ball M, Andrews SP, Wierschem F, Cleator E, Smith MD, Ley SV: Total synthesis of thapsigargin, a potent SERCA pump inhibitor. *Org Lett* **2007**, 9:663-666
4. Youn UJ, Miklossy G, Chai X, Wongwiwatthananut S, Toyama O, Songsak T, Turkson J, Chang LC: Bioactive sesquiterpene lactones and other compounds isolated from *Vernonia cinerea*. *Fitoterapia* **2014**, 93:194-200

Supplementary Figures

Fig. S1

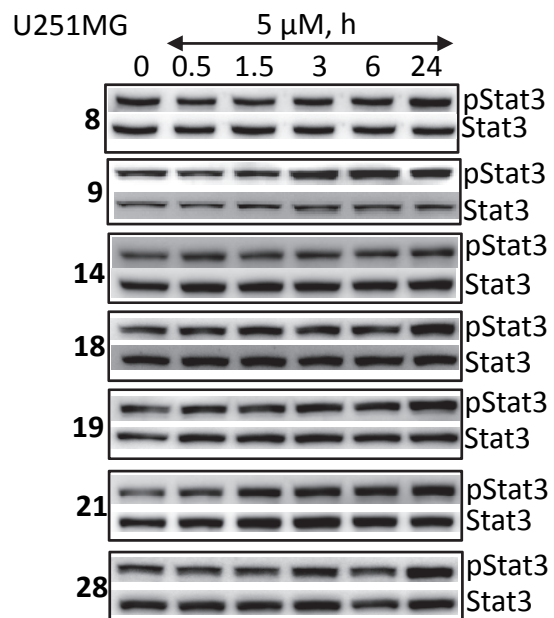


Figure S1. **Hirsutinolides inhibit Stat3 activation in tumor cells.** U251MG cells in culture were treated with 5 μ M **8**, **14**, **18**, **19**, **21** or **28**, and whole-cell lysates of equal total protein prepared and subjected to immunoblotting analysis for pY705Stat3 and Stat3. Positions of proteins in gel are labeled; control lane (0) represents whole-cell lysates prepared from cells treated with 0.025% DMSO. Data are representative of 2-3 independent determinations.

Fig. S2.

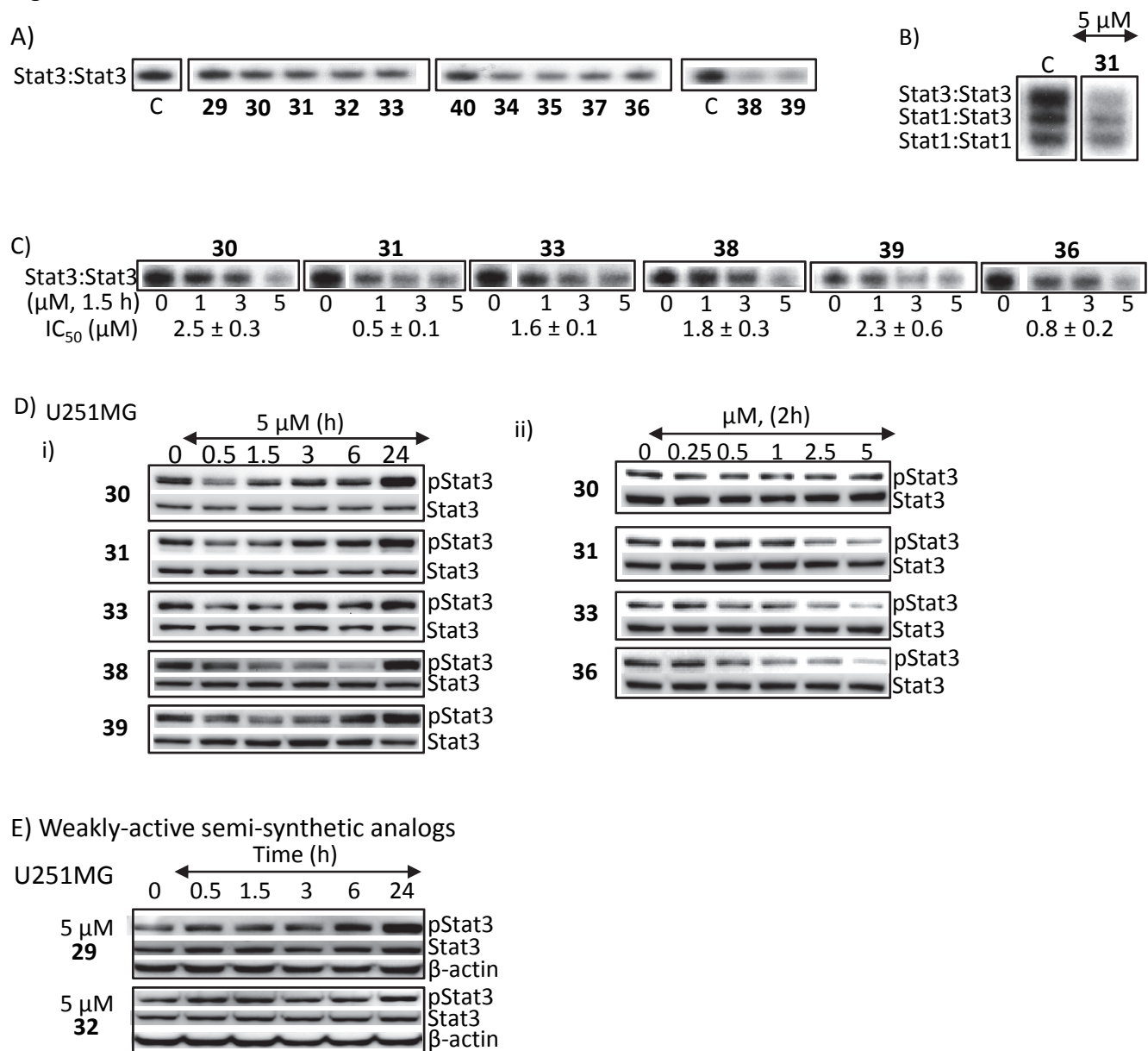


Figure S2. Semi-synthetic analogs inhibit Stat3 activation. (A-C) Nuclear extracts containing activated (A and B) Stat3 from NIH3T3/v-Src fibroblasts or (C) Stat1 and Stat3 from EGF-stimulated NIH3T3/hEGFR were pre-incubated with the designated semi-synthetic analogs for 30 min at room temperature prior to incubating with the radiolabeled hSIE probe that binds Stat1 and Stat3 and performing EMSA analysis; (D and E) Immunoblotting analysis of whole-cell lysates prepared from U251MG cells treated with the designated compounds at (D(i) and E) 5 μ M for 0-24 h or (D(ii)) 0-5 μ M for 2 h and probing for pStat3, Stat3 or β -actin. Positions of proteins or Stats:DNA complex in gel are labeled; control lane (c, 0) represents whole-cell lysates or nuclear extracts prepared from 0.025% DMSO-treated cells or nuclear extracts pre-treated with 0.025% DMSO. Bands corresponding to Stats:DNA complexes were scanned and quantified using ImageJ, plotted against concentration of agent from which IC₅₀ values were derived. Data are representative of 2-3 independent determinations.

Fig. S3

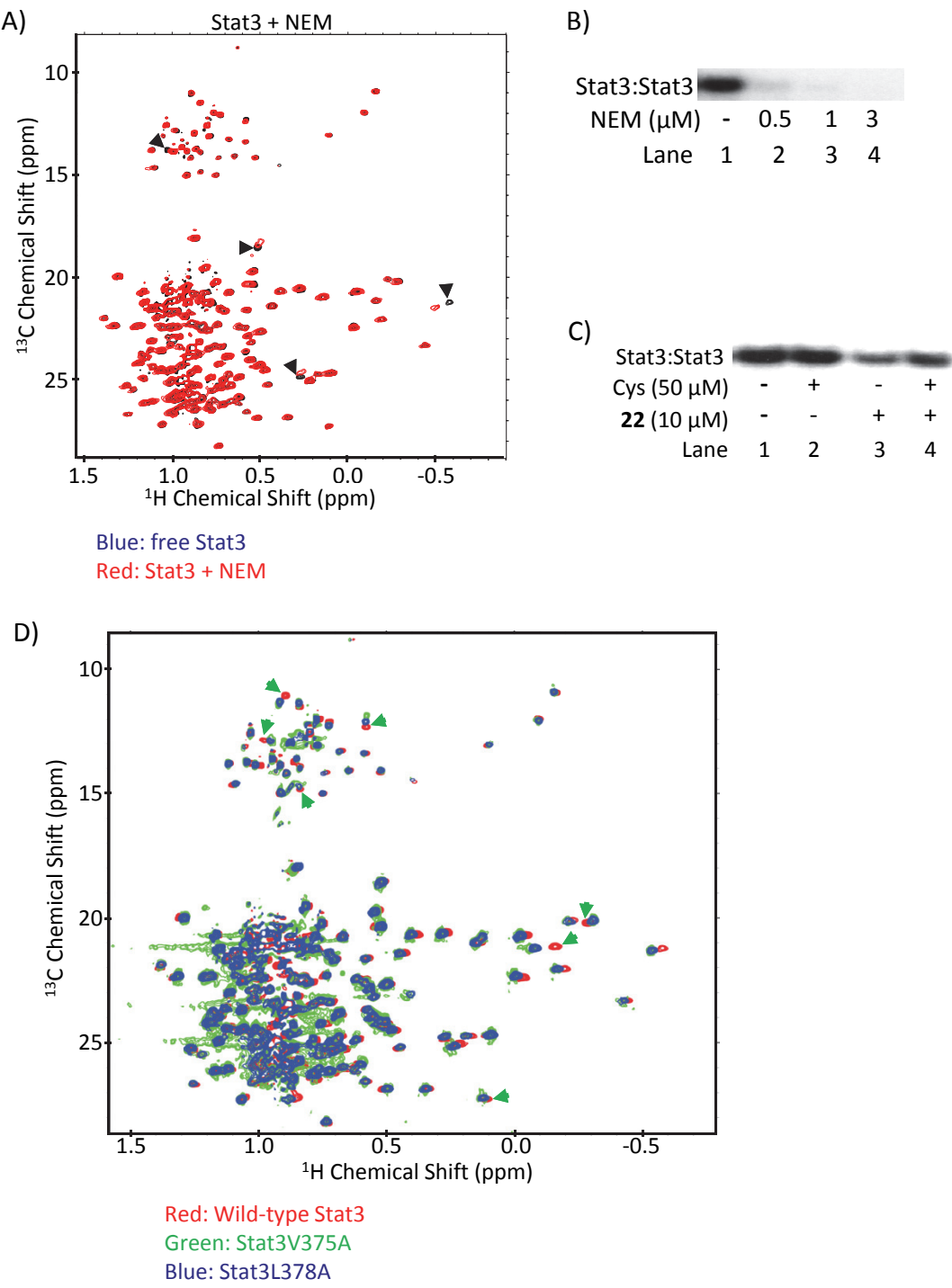
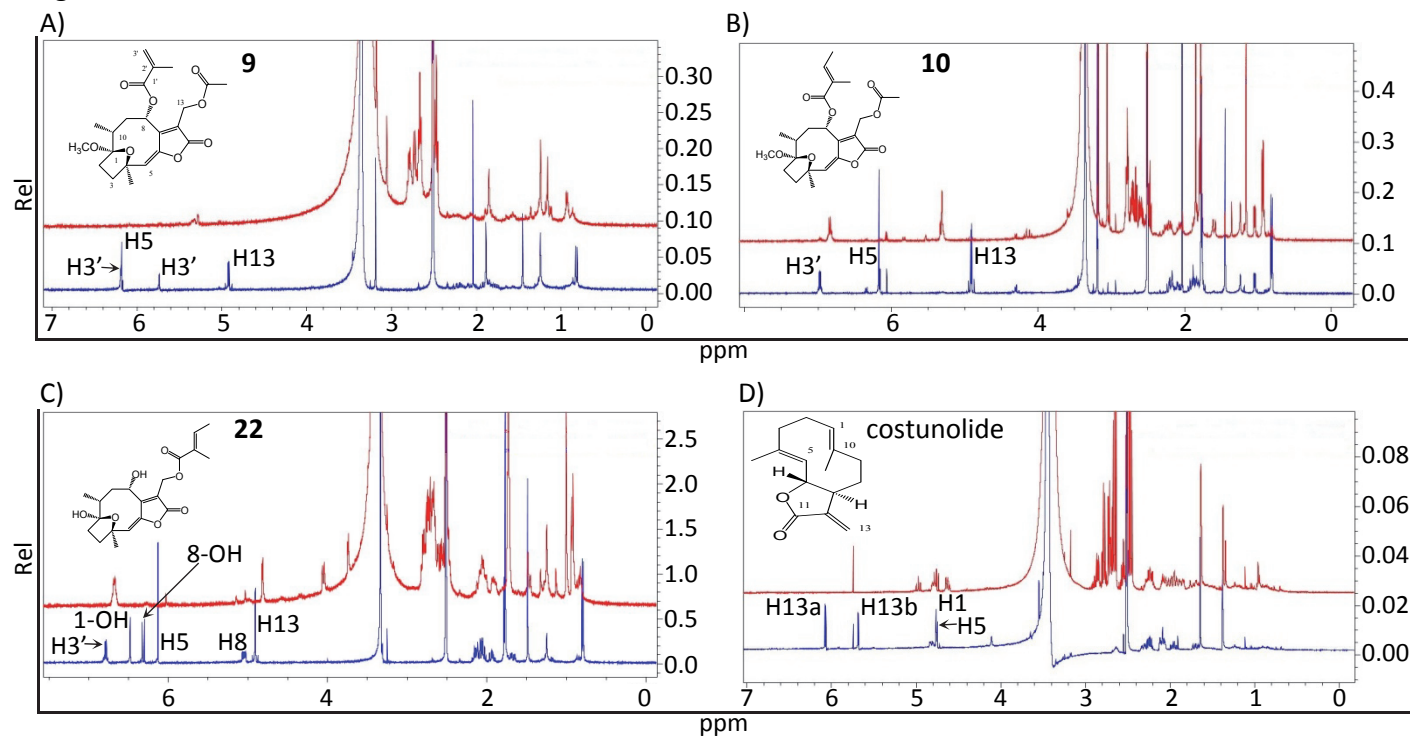


Figure S3. NMR analysis of wild-type and mutated Stat3 in solution with or without NEM and Stat3 DNA-binding activity and the effects of NEM or 22 in the presence or absence of Cysteine. (A) Overlay of the ^1H - ^{13}C HMQC spectra of wild-type Stat3, free (black) or wild-type Stat3 in the presence of NEM (red) showing residues with significant changes in either resonance line-widths or NMR chemical shifts that are indicated by arrowheads; (B and C) Stat3 DNA-binding assay of nuclear extracts prepared from NIH3T3/v-Src fibroblasts containing activated Stat3 pre-incubated for 30 min with (B) 0-3 μM NEM or (C) 10 μM **22** in the presence or absence of 50 μM cysteine (Cys) prior to incubation with the radiolabeled hSIE probe that binds Stat3 and subjecting to EMSA analysis; and (D) Overlay of the ^1H - ^{13}C HMQC spectra of Stat3, wild-type (red) and mutant Stat3V375A (green) and Stat3L378A (blue). NEM-induced peak shifts or similar types are indicated by black arrowheads; peaks that are shifted and not due to treatment with NEM are indicated by green arrowheads. Positions of Stat3:DNA complex in gel are labeled; control lane (-) represents nuclear extracts pre-treated with 0.025% DMSO. Data are representative of 2-3 independent determinations.

Fig. S4



Blue: Compound alone

Red: Compound + 2 molar equivalent of cysteamine

Figure S4. ^1H NMR spectra of (A) **9**, (B) **10**, (C) **22** and (D) costunolide in $\text{DMSO-}d_6$ and the effects of the reactions with cysteamine (red) compared to compound alone control (blue). Data are representative of 2 independent determinations.

Fig. S5.

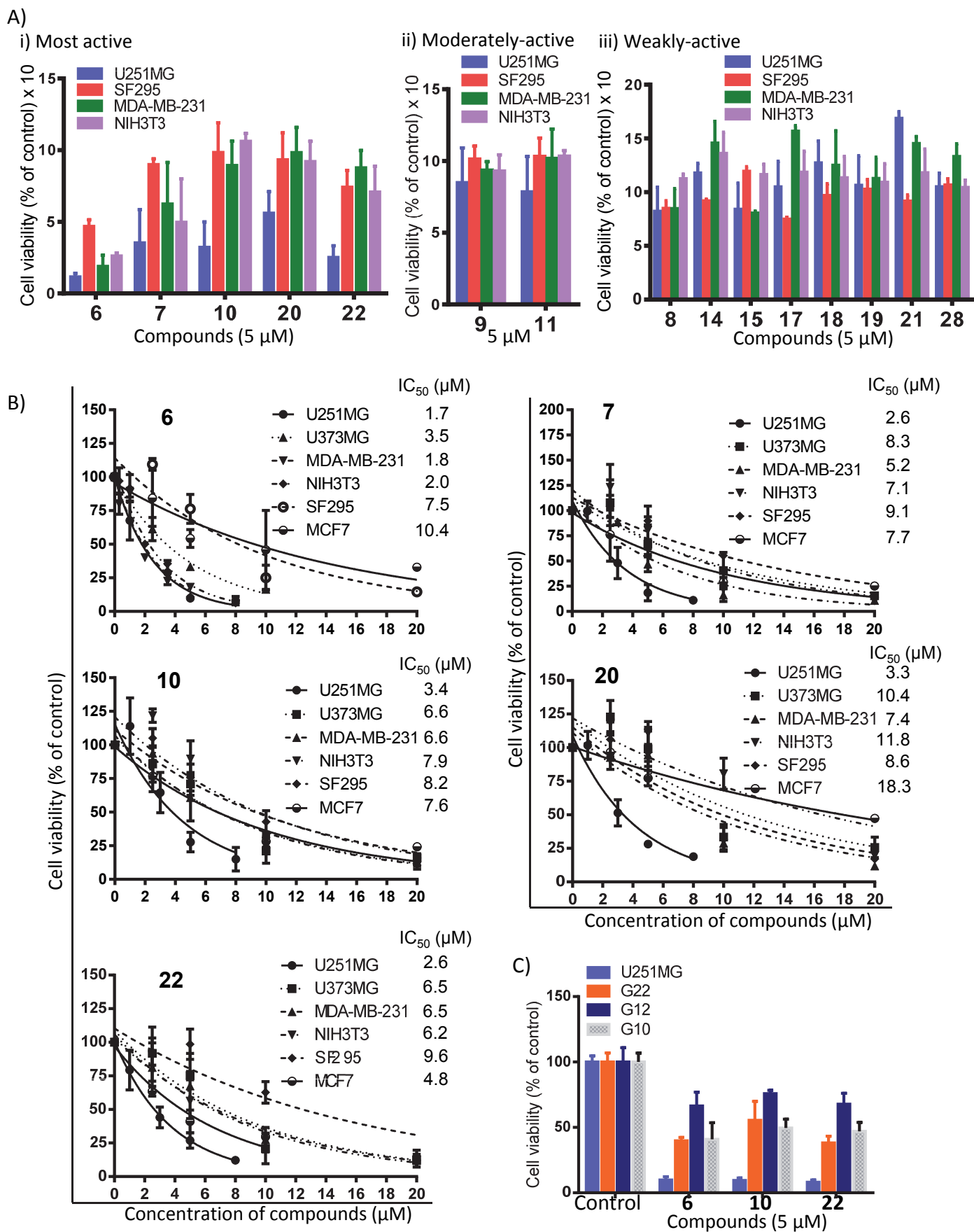
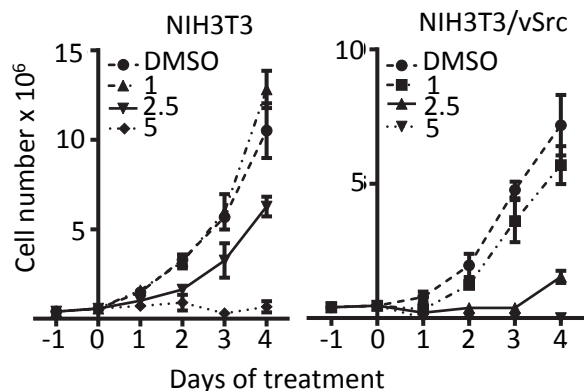
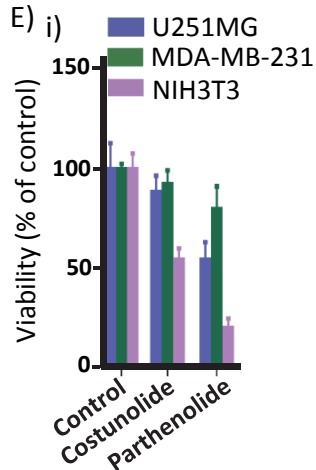


Fig. S5.

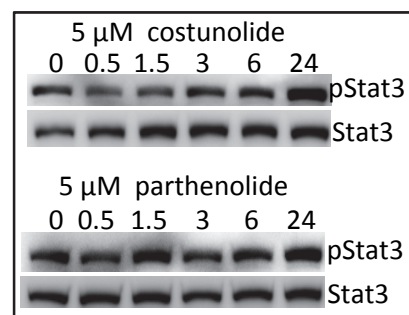
D)



E) i)

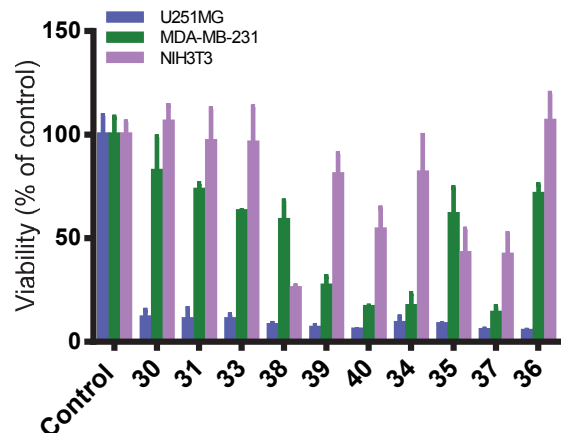


ii)

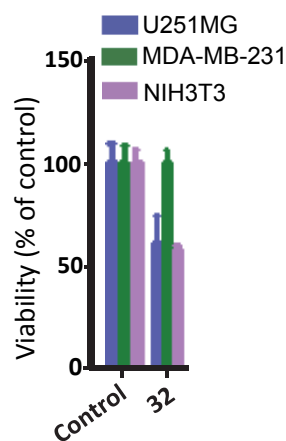


F) Semi-synthesized analogs

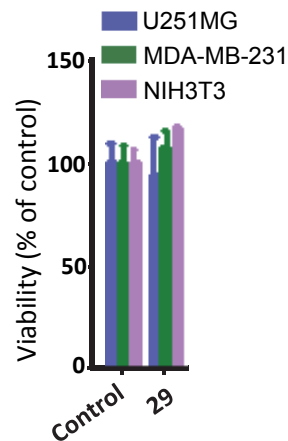
i) Most active



ii) Moderately active



iii) Weakly active



G) Dose-response studies of semi-synthesized analogs

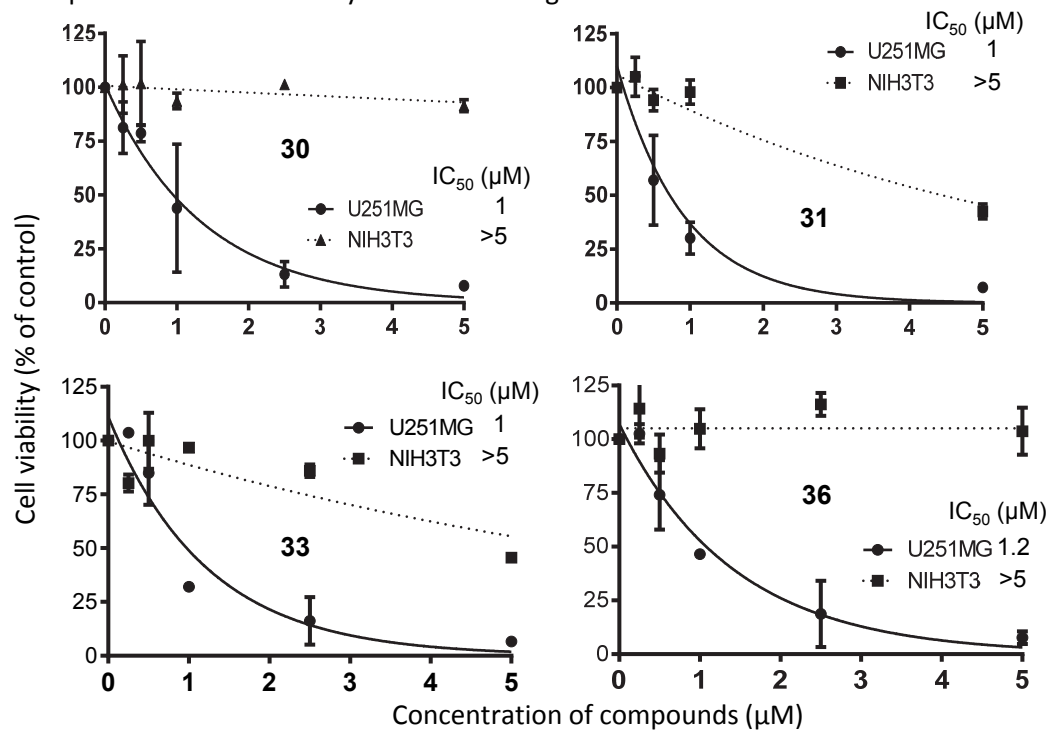


Fig. S5.

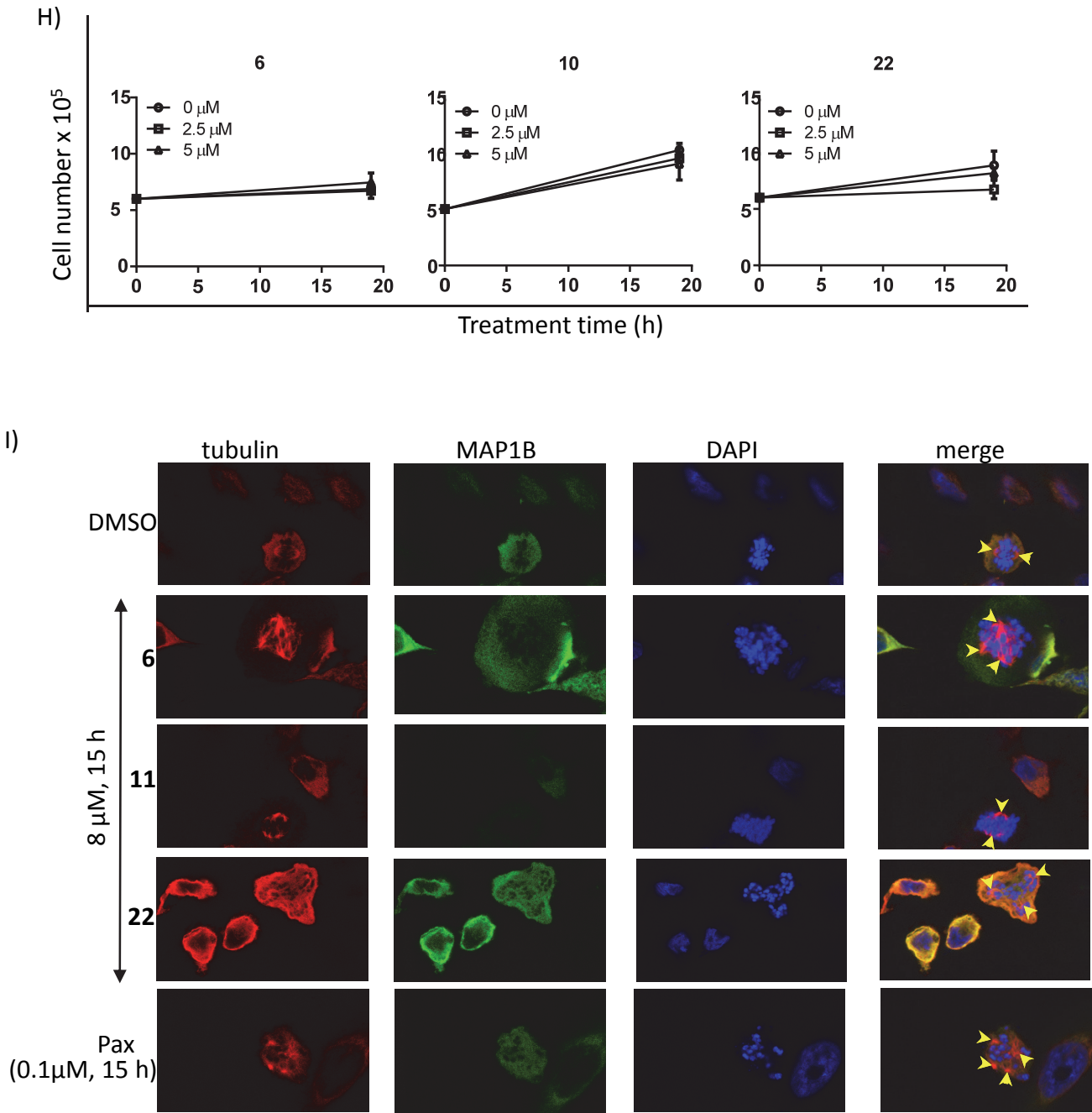
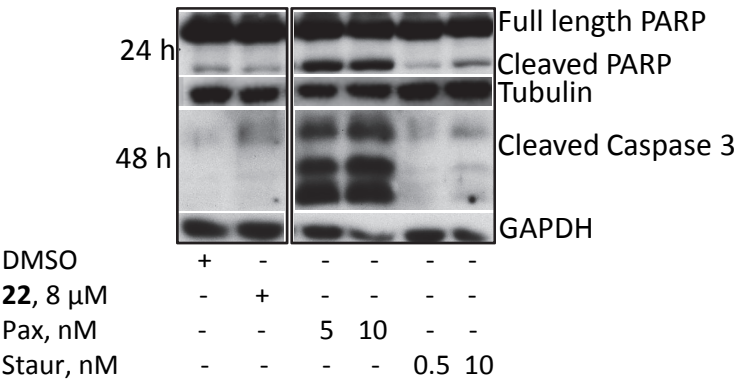


Fig. S5.

J)



K)

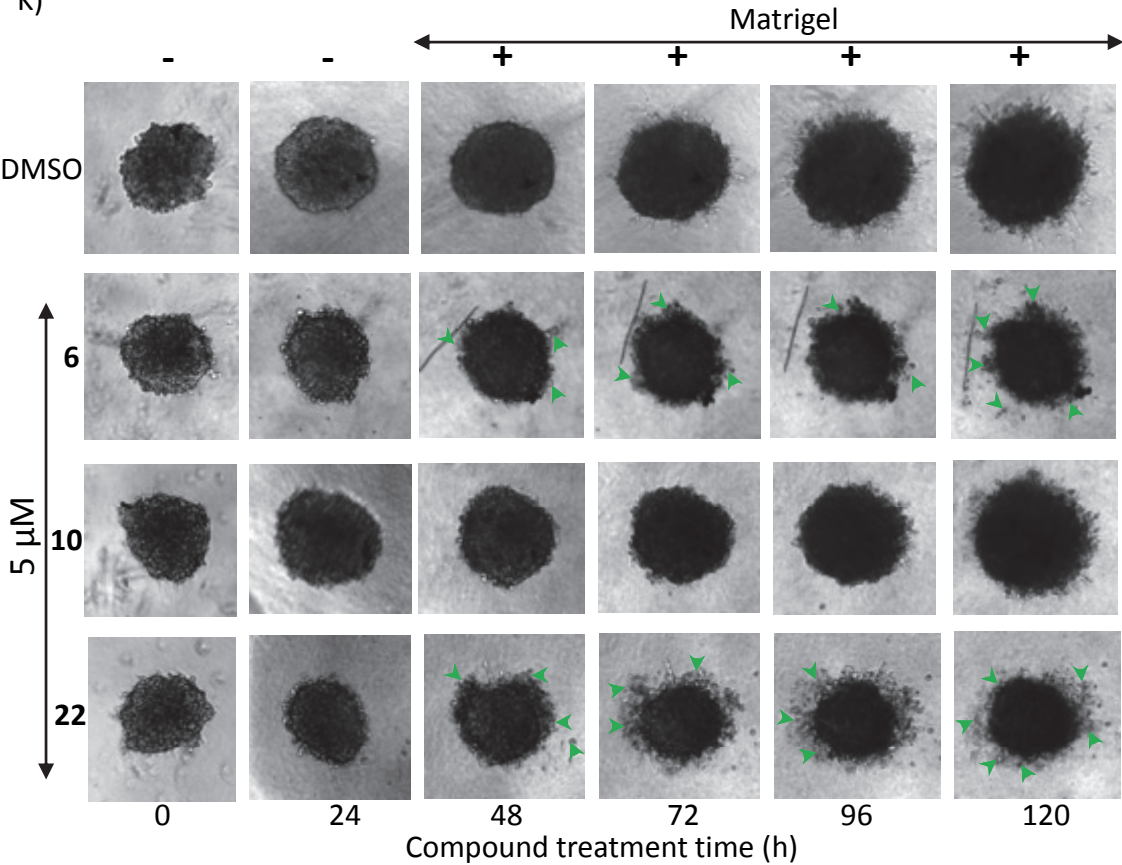


Figure S5. Effects of hirsutinolides or semi-synthetic analogs on growth and viability of glioma cells in culture and as 3D spheroids. (A-C) Cell viability plots for the effects on (A and B) human tumor or mouse cell lines and (C) patient-derived xenograft cells, G22 of 72-h treatments with (A) the designated hirsutinolides at 5 μ M, (B) 0-20 μ M **6**, **7**, **10**, **20** or **22**, and (C) 5 μ M **6**, **10** or **22**. Insert, IC₅₀ values determined from the dose-response curves; (D) Trypan blue exclusion/phase contrast microscopy for viable cell numbers and the effect of treatment with 0-5 μ M **22** over four days; (E) Effect of 5 μ M costunolide or parthenolide on the (i) viability of the indicated cell lines following 72-h treatment, or (ii) pStat3 and Stat3 levels, measured by immunoblotting analysis of whole-cell lysates from U251MG cells following 0-24 h treatment; (F and G) Cell viability plots for the effects of 72-h treatments with (F) 5 μ M of the designated analogs on the indicated human tumor or mouse cell lines, and (G) 0-5 μ M of the designated analogs on U251MG cells. Insert, IC₅₀ values determined from the dose-response curves; (H) U251MG cells in culture were treated once with 0-5 μ M **6**, **10** or **22** and viable cell numbers at 19 h post-treatment were counted and plotted; (I) U251MG cells growing on glass cover slips were synchronized by double thymidine block, released, and treated or untreated with the designated compounds for 15 h and processed for confocal microscopy imaging analysis of β -tubulin, MAP1B, and DAPI using a Leica TCS SP5 confocal microscope. Images were captured and processed using LAS AF Lite software; Yellow arrowheads indicate poles; (J) Immunoblots of poly ADP ribose polymerase (PARP), caspase, tubulin and GAPDH and the effects of treatment with **22**, paclitaxel (Pax), and staurosporine (Staur) at the designated concentrations for 24 or 48 h; and (K) Human glioma patient-derived xenograft cells, G22 growing as 3D spheroids formed over a 48-h duration, were untreated (DMSO) or treated once with 5 μ M **6**, **10** or **22** for 24 h prior to (-) the addition of matrigel (+), and allowed to grow for up to 120 h and imaged at 24 h intervals, which are shown. Green arrowheads indicate areas of extensive disaggregation. Positions of proteins in gel are labeled; control lane (-, 0) represents whole-cell lysates or cells treated with 0.025% DMSO. Data are representative of 2-4 independent determinations. Values are the mean \pm S.D, n=3-4.

Fig. S6.

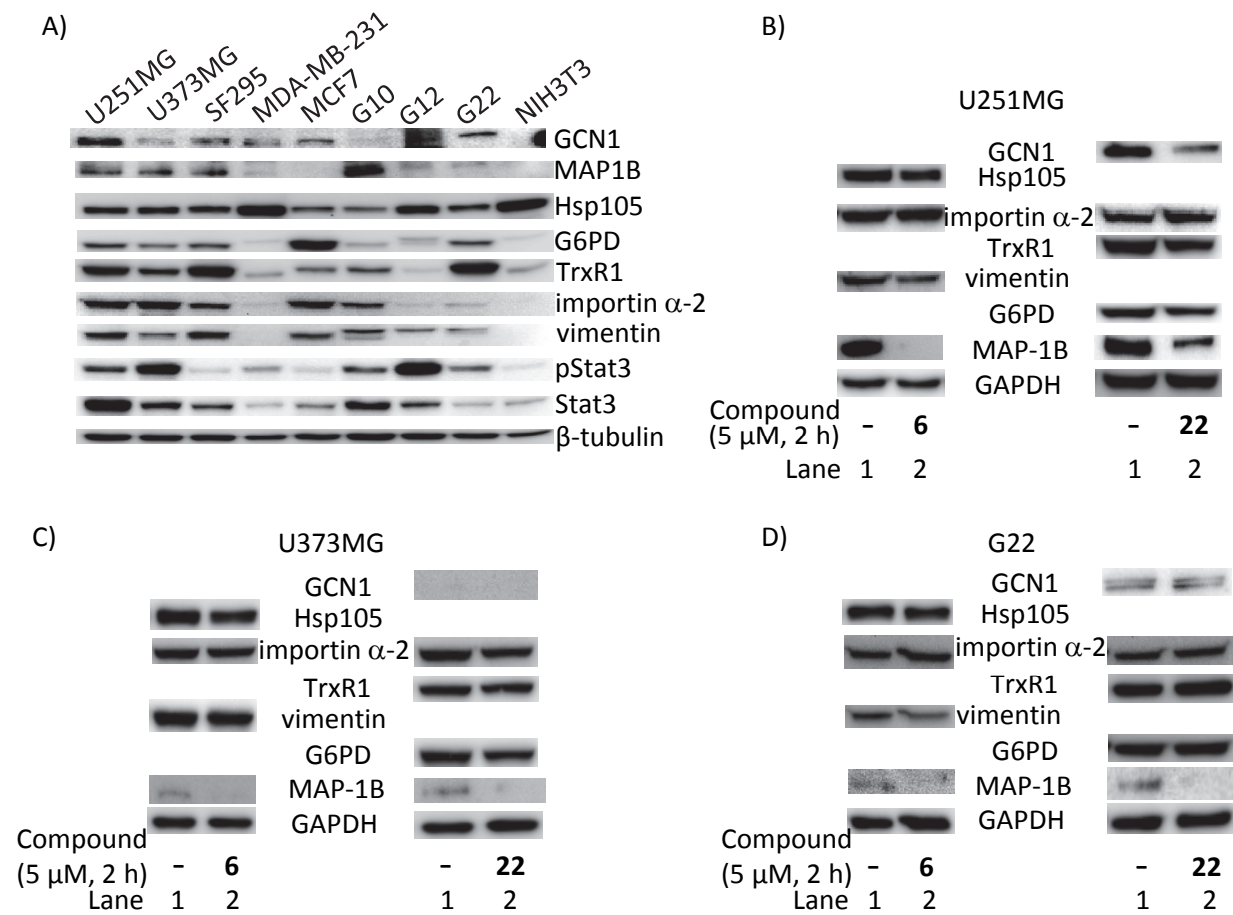


Figure S6. **Hirsutinolides modulate GCN1, Hsp105, importin α -2, vimentin, G6PD, TrxR1 or MAP1B protein expression.** (A-D) Hsp105, importin subunit α -2, vimentin, TrxR1, GCN1, G6PD, MAP1B, GAPDH, and β -tubulin immunoblots in whole-cell lysates from the designated cell lines and patient-derived xenograft cells (A) untreated or (B-D) treated with 5 μ M **6** or **22** for 2 h. Positions of proteins in gel are labeled; control lane (-) represents whole-cell lysates prepared from 0.025% DMSO-treated cells. Data are representative of 3 independent determinations.

Fig. S7.

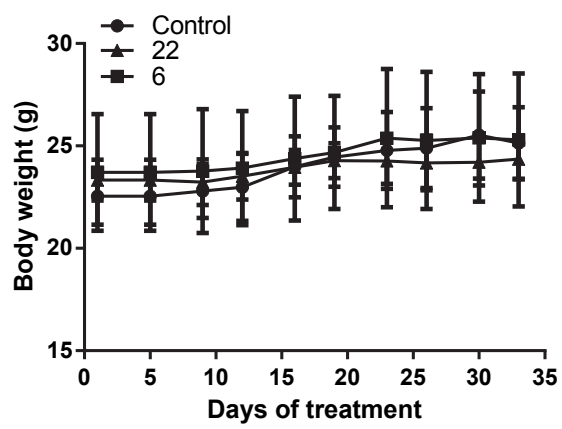


Figure S7. **Body weights of tumor-bearing mice treated with hirsutinolides.** Plots of body weight against days of treatment for mice bearing human glioma (U251MG) tumors and treated with **6** or **22** via oral gavage, 2 mg/kg or vehicle (1% DMSO) every other day for the indicated times. Body weights of mice were measured every 3-4 days and plotted.